Materials Science-Poland, 32(4), 2014, pp. 541-546
http://www.materialsscience.pwr.wroc.pl/
DOI: 10.2478/s13536-014-0246-5

VERSITA

Preparation and microstructural characterization of Si(100) $Ce_{1-x}Gd_xO_{2-\delta}$ thin films prepared by pulsed laser deposition technique

P. NAGARAJU[1]*, Y. VIJAYAKUMAR[2], D.M. PHASE[3], V.R. REDDY[3], M.V. RAMANA REDDY[2]

[1]CMR Technical Campus, Hyderabad, India
[2]Department of Physics, Osmania University, Hyderabad, India
[3]IUC, Indore, India

Microstructural properties of $Ce_{1-x}Gd_xO_{2-\delta}$ (x = 0 to 0.3) thin films prepared by pulsed laser deposition technique were studied. The thin films were deposited on Si(100) substrate at a substrate temperature of 973 K at the oxygen partial pressure of 0.2 Pa using KrF excimer laser with energy of 220 mJ. The prepared thin films were characterized by X-ray diffraction, Raman spectroscopy and atomic force microscopy. X-ray diffraction analysis confirmed the polycrystalline nature of the thin films. Crystallite size, strain and dislocation density were calculated. The Raman studies revealed the formation of Ce–O with the systematic variation of peak intensity and full width half maxima depending on concentration of gadolinium dopant. The thickness of the films was estimated using Talystep profiler. The surface roughness was estiamted based on AFM.

Keywords: *cerium oxide; dislocation densities; gadolinium doped cerium oxide; microstructure; pulsed laser deposition; thin films.*

© Wroclaw University of Technology.

1. Introduction

Cerium oxide and gadolinium doped cerium oxide thin films are attracting great attention in technological applications. High refractive index, absorption of UV radiation, transparency in the visible and near-IR region, make cerium oxide thin films an ideal UV blocker and excellent substitute for titanium oxide and zinc oxide in sunscreens [1–5]. Cerium oxide plays an important role in electrochromic devices [6] as a substrate for high temperature superconductors [7], silicon-on-insulator (SOI) structures [8, 9], miniaturized capacitors [10, 11], counter electrode in smart windows due to its high transparency [12, 13]. Various techniques have been employed to prepare cerium oxide and gadolinium doped cerium oxide thin films, such as sol-gel method [14], sputtering [15], electron beam evaporation [16], metal organic chemical vapor deposition [17], atomic layer deposition [18], spray pyrolysis [19] and pulsed laser deposition (PLD) [20–23]. Pulsed laser deposition is the most predominant method of all aforesaid techniques as it produces layers with high uniformity, good stoichiometry as well as free from contamination, which could arise during the deposition process. It is the most effective method to prepare extremely pure film.

This method can be successfully adopted to prepare multi-component material that is difficult to process in a thin film form by any other method. Cerium oxide is an electrical insulator with the fluorite structure and a lattice constant of 0.539 nm. However, its ionic conductivity can be improved by an appropriate doping. It was reported that in a bulk form the conductivity of ceria can be remarkably enhanced by increasing the concentration of oxygen vacancies after doping with gadolinium at fixed doping concentrations. Among the rare-earth doped ceria, the radius of Gd dopant ion is close to that of the host cation [24]. Hence, great attention has been paid on the doping of ceria by Gd to

*E-mail: nagarajuphysics@gmail.com

bring an improvement in structural and morphological properties.

2. Experimental

Cerium ammonium nitrate ($Ce(NH_4)_2(NO_3)_6$ and gadolinium nitrate ($Gd(NO_3)_3$, 99.99 %, were used as starting precursors, citric acid and ethylene glycol were selected for the polymerization treatment. Nitrates were dissolved in deionized water separately and then the solutions were mixed in a beaker. Citric acid was dissolved in deionized water and then added to the cation solution. The molar ratio of total nitrates: citric acid and ethylene glycol: citric acid was taken as 2:1 and 4:1, respectively. After homogenization of this solution, temperature was raised to 353 K and the solution was kept for 6 hours at this temperature on a magnetic stirrer to remove additional water. The obtained gel was cooled down to room temperature. Then, the compound was dried at 393 K for 24 hours. Finally, the prepared powder was calcined at 1673 K for 8 hours. The sol-gel prepared compound $Ce_{1-x}Gd_xO_{2-\delta}$ ($x = 0, 0.1, 0.2$ and 0.3) was formed into pellets with 20 mm of diameter and 5 mm of thickness at a pressure of 294.2 MPa by using a hydraulic pelletizer. The prepared pellets were again sintered at 1673 K for 8 hours. Block diagram of pulsed laser deposition process is shown in Fig. 1.

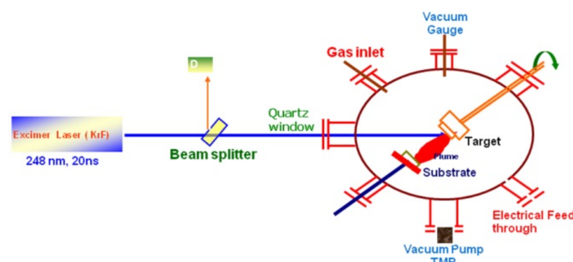

Fig. 1. Block diagram of PLD evaporation process.

In the pulsed laser deposition system, a laser beam is generated outside the chamber. Also the optical instruments, like lenses, mirrors and apertures, whose objective is to guide and focus the laser beam, are placed before the port of the deposition chamber. In the chamber the laser beam is directed towards the target. The absorption of the laser radiation is followed by breaking of chemical bonds in the target material and ablation of atoms, ions, electrons, molecules, atomic clusters and even bigger particles. These evaporated species form a plasma plume, which expands in the vacuum and flows towards the substrate to form the deposit. Deposition parameters are shown in the Table 1.

Table 1. Deposition parameters for PLD.

Substrate:	Si(100)
Laser:	KrF excimer
Wavelength:	248 nm
Pulse repetition rate:	10 Hz
Oxygen partial pressure:	0.2 Pa
Source-substrate distance:	4 cm
Substrate Temperature:	973 K
Laser Energy:	220 mJ
Deposition time:	30 min.

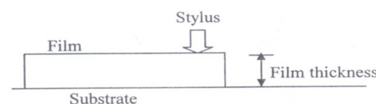

Fig. 2. The idea of measurement with Tallystep profiler.

3. Results and discussion

3.1. Thickness measurement

After deposition, thickness of the thin films was measured by Tallystep measurement technique. Tallystep is a stylus instrument for thickness measurement of thin film deposits, having a range of applications in micro-topography and metallurgical research. The stylus is traversed over the film surface shown in Fig. 2. While deposition of a film, there is some part of the substrate, where no deposition takes place. The boundary line between the deposited and undeposited portion forms something like a step on the substrate surface. When the stylus, moving over the film, comes to this region, it experiences the change or difference in height. Vertical movement of the stylus is amplified electronically and recorded as graphical representation

of the differences at the level between the surface of the substrate and the deposit. Film thickness of cerium oxide (x = 0) and gadolinium doped cerium oxide (x = 0.1, 0.2 and 0.3) was found to be 400 nm.

3.2. G.I. XRD

The microstructural properties of the $Ce_{1-x}Gd_xO_{2-\delta}$ (x = 0 to 0.3) thin films were investigated by high resolution X-ray diffraction system (G.I X-ray diffraction) using a LiF monochromator with 15.4 nm wavelength in the range of 20° to 60° with 1°/min scanning speed. Fig. 3 shows a typical XRD pattern of the $Ce_{1-x}Gd_xO_{2-\delta}$ (x = 0 to 0.3) thin films deposited on Si(100) at 973 K. Three different orientations of thin films at (111), (220) and (311) planes are observed.

These diffraction planes are in a good agreement with JCPDF data. In the present work the (111) diffraction planes reveal the highest peak intensities compared to other peaks in pure and Gd doped ceria thin films. Based on this it is considered that the growth of the film takes place along (111) plane. The XRD spectra show that the same crystal structure was attained for pure ceria and Gd doped ceria thin films. As the ionic radii of Ce^{4+} and Gd^{3+} are 0.111 and 0.119 nm, respectively, it can be predicted that Gd ions are probably placed in Ce positions in the crystal lattice. The average crystallite size D of cerium oxide and gadolinium doped cerium oxide thin films were estimated for (111) plane with the help of Sherrer's formula [25]:

$$D = \frac{0.94\lambda}{\beta \cos\theta} \tag{1}$$

where λ is the wavelength (15.4 nm) of incident beam, β is the intrinsic width at half maximum of (hkl) peak, and θ is the Bragg's diffraction angle.

It is clear that the average crystallite size is much finer for pure cerium oxide thin films than that of gadolinium doped cerium oxide thin films. The variation of crystallite size with gadolinium concentration in ceria is shown in Fig. 4.

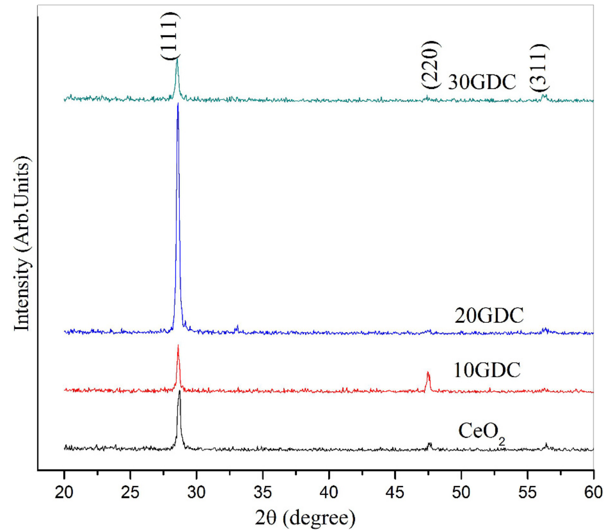

Fig. 3. XRD pattern of the cerium oxide and gadolinium doped cerium oxide thin films deposited on Si(100) substrate.

The strain and dislocation density was calculated using the formula [26]:

$$(\varepsilon) = \frac{\beta \cos\theta}{4} \tag{2}$$

The dislocation density (δ), defined as the length of dislocation lines per unit volume, is given by:

$$(\delta) = 1/D^2 \tag{3}$$

For pure cerium oxide thin films, the dislocation density and strain was found to be maximum, whereas for 10GDC thin films these values were minimal. With an increase in Gd concentration in cerium oxide the dislocation density and strain have increased. The decrease in dislocation density indicates the formation of films of high quality [27]. The inhomogeneous strain component is localized at the sub grain and sub domain level near grain boundaries [28].

3.3. Raman spectroscopy

The Raman spectra for cerium oxide, 10GDC, 20GDC and 30GDC thin films were recorded using Jobin Yvon Horibra LABRAM-HR visible (400 to 1100 nm) spectrometer in the spectral

Table 2. Structural parameters of pure ceria and Gd doped ceria thin films.

Sample	d-spacing (nm)		Lattice constant (nm)	
	Deposited	JCPDF	Deposited	JCPDF
CeO_2	0.310	0.312	0.538	0.541
$Ce_{0.9}Gd_{0.1}O_{1.95}$(10GDC)	0.311	0.312	0.539	0.541
$Ce_{0.8}Gd_{0.2}O_{1.90}$(20GDC)	0.311	0.313	0.539	0.542
$Ce_{0.7}Gd_{0.3}O_{1.85}$ (30GDC)	0.312	0.313	0.540	0.542

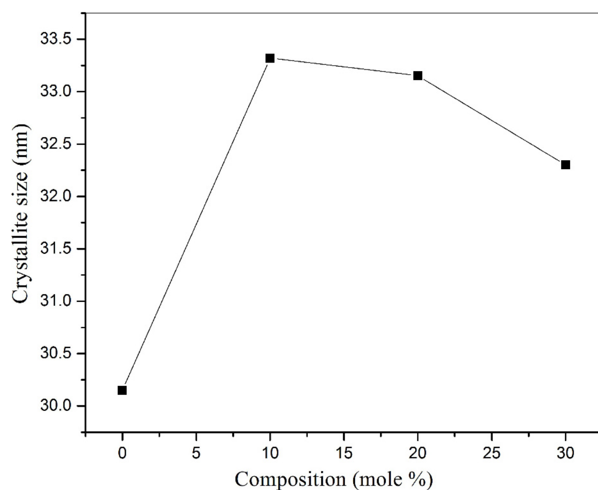

Fig. 4. Variation of crystallite size with gadolinium concentration in cerium oxide thin films.

d-spacing was calculated by using Bragg's equation, 2dsinθ = nλ. Calculated lattice constant is in good agreement with JCPDF data (81-0792), (75-0161), (75-0162) and (75-163) for cerium oxide, 10GDC, 20 GDC and 30 GDC thin film, respectively. Calculated d-spacing and lattice constant values are shown in the Table 2.

range of 100 to 800 cm^{-1} at the room temperature (Fig. 6). An intense vibrational mode at 463 cm^{-1} is due to the F_{2g} symmetry of CeO_2, i.e. symmetric breathing mode of oxygen atoms around the cerium ions [29, 30]. Replacement of Ce^{4+} with Gd^{3+} at the lattice site results from breaking of the Ce–O bond with creation of oxygen vacancies. Thus, besides F_{2g} mode, few additional modes in the region between 550 cm^{-1} and 700 cm^{-1} can be observed. The band at 518 cm^{-1}, observed in all the cases, is due to substrate of Si wafer. As the concentration of Gd increases, a decrease in intensity of the peak and broadening of Raman shift is observed.

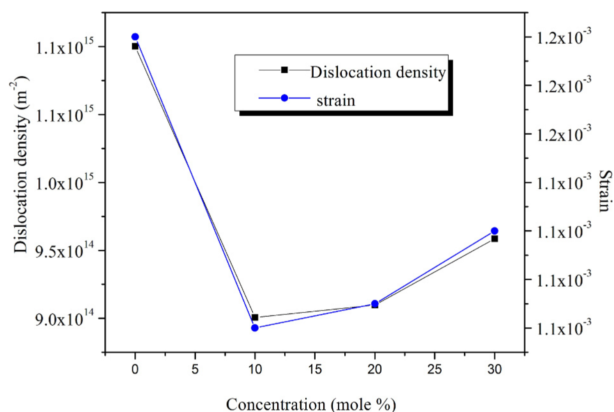

Fig. 5. Variation of strain and dislocation density of $Ce_{1-x}Gd_xO_{2-\delta}$ (x = 0 to 0.3) thin films with Gd concentration.

The Raman shift for doped ceria is slightly different due to variation in bond length, atomic geometry and lattice spacing of ceria on doping.

3.4. Atomic force microscopy

Atomic force microscopy study was carried out to investigate the surface morphology and surface roughness of the ceria and Gd doped ceria thin films deposited on Si wafer (100) substrate. Fig. 7 shows the AFM images of Ceria, 10GDC, 20GDC and 30GDC thin films. The surface roughness was quantitatively measured by the RMS (root mean square) roughness. The surface roughness of the pure ceria thin films was found to be maximum. On the other hand, in Gd doped cerium oxide thin films, while the doping concentration is increasing from 10 mol % to 30 mol %, the RMS roughness increases, which may be due to different kinetics of the doped atoms and the host atoms on the surface of the thin film. All the thin films were

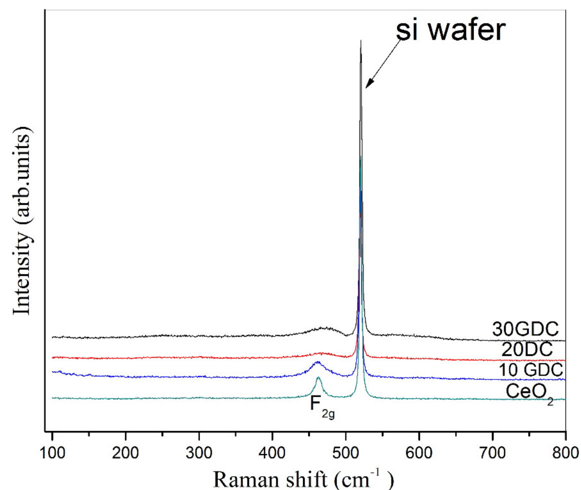

Fig. 6. Raman spectra of ceria and Gd doped ceria thin films.

prepared under the same conditions at 973 K, however, significant change in their surface morphologies has been observed with increasing concentration of Gd. Both an increase in the value of crystallite size and in the RMS roughness of the films occurred. The variation of RMS roughness with concentration of Gd is shown in Table 3. Dislocation densities of the thin films are also in good agreement with AFM analyses.

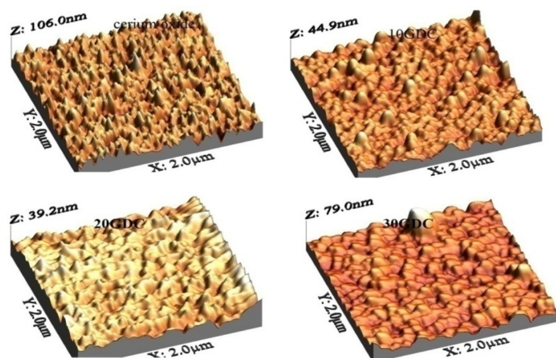

Fig. 7. AFM images of cerium oxide and Gd doped cerium oxide thin films.

4. Conclusions

Pure and Gd doped cerium oxide thin films were prepared using 220 mJ laser energy on Si(100) at a substrate temperature of 973 K. The thin films were found to be polycrystalline with (111) orientation. The crystallite size was found to be in the range of 30 to 35 nm and was not much affected due to Gd. Dislocation density and strain were calculated for cerium oxide, 10GDC, 20GDC and 30GDC. It was found that for 10GDC thin films dislocation density and strain was less in comparison with the remaining Gd doped ceria thin films. It indicates that good quality and homogeneous thin films can be prepared with 10GDC. The Raman peak at 463 cm^{-1} indicates the F_{2g} active mode. The atomic force microscope investigation indicates that the RMS roughness is minimum for 10GDC thin films compared with the other Gd doped cerium oxide thin films.

Table 3. Surface morphology of pure and Gd doped cerium oxide thin films.

No.	Sample	Surface roughness (nm)
1	CeO_2	12.55
2	$Ce_{0.9}Gd_{0.1}O_{1.95}$ (10GDC)	4.25
3	$Ce_{0.8}Gd_{0.2}O_{1.90}$ (20GDC)	4.35
4	$Ce_{0.7}Gd_{0.3}O_{1.85}$ (30GDC)	7.58

Acknowledgements

The authors would like to thank Dr. V. Ganesan, IUC, Indore, for providing AFM facility, and also thank the management of CMR technical campus for constant encouragement to carry out this work.

References

[1] YABE S., SATO T., *J. Solid State Chem.*, 171 (2003), 7.
[2] SAINZ M.A., DURAN A., FERNADEZ-NAVARRO J.M., *J. Non-Cryst. Solids*, 121 (1990), 315.
[3] AL-ROBAEE M.S., RAO K.N., MOHAN S., *J. Appl. Phys.*, 71 (1992), 2380.
[4] ZHENGG S.-Y., ANDERSSON-FÄLDT A.M., STJERNA, GRANQVIT C.G., *Appl. Optics*, 32 (1993), 6303.
[5] GHANASHYAM KRISHNA M., HARTIDE A., BHATTACHARYA A.K., *Mater. Sci. Eng. B-Adv.*, 55 (1998), 14.
[6] OZER N., *Sol. Energ. Mat. Sol. C.*, 68 (2001), 391.
[7] PHILLIPS J.M., *J. Appl. Phys.*, 79 (1996), 1829.
[8] CHIKYOW T., BEDAIR S.M., TYE L., ELMASRY N.A., *Appl. Phys. Lett.*, 65 (1994), 1030.
[9] SUZUKI M., AMI T., *Mater. Sci. Eng. B-Adv.*, 41 (1996), 166.

[10] NAKAZAWA T., INOUE T., SATOH M., YAMAMOTO Y., *Jpn. J. Appl. Phys.*, 34 (1995), 548.

[11] ROH Y.H., KIM K., JUNG D.G., *Jpn J. Appl. Phys.*, 36 (1997), L1681.

[12] GRANQVIST C.G, AZENS A., HJELM A., KULLMAN L., NIKLASSON G.A., RONNOW D., STROMME-MATTSSON M., VAIVARS G., *Sol. Energy*, 63 (1998), 199.

[13] ELIDRISSI B., ADDOU M., REGRAGUI M., MONTY C., KACHOUANE A., *Thin Solid Films*, 379 (2000), 23.

[14] NILGUN O., *Sol. Energ. Mat. Sol. C.*, 68 (2001), 391.

[15] STROMME-MATTSON M., AZENS A., NIKLASSON G.A., GRANQVIST C.G., PURANS J., *J. Appl. Phys.*, 81 (1997), 6432.

[16] HONG S., KIM S.H., KIM W.J, YOON H.H., *Curr. Appl. Phys.*, 11 (2011), 163.

[17] GRABOY I.E., MARKOV N.V., MALEEV V.V., KAUL A.R., POLYAKOV S.N., SVETCHNIKOV V.L., ZANDBERGEN H.W., DAHMEN K.H., *J. Alloy. Compd.*, 251 (1997), 318.

[18] PAIVASAARI J., PUTKONEN M., NIINISTO L., *J. Mater. Chem.*, 12 (2002), 1828.

[19] ELIDRISSI B., ADDOU M., REGRAGUI M., MONTY C., BOUGRINE A., KACHOUANE A., *Thin Solid Films*, (2000), 379.

[20] MUTHUKKUMARAN K., KUPPUSAMI P., MATHEWS, MOHANDAS E., SELLADURAI S., *Mater. Sci.-Poland.*, 25 (2007), 671.

[21] COSSARUTTO L., CHAOUI N., MILLON E., MULLER J.F., LAMBERT J., ALNOT M., *Appl. Surf. Sci.*, 126 (1998), 352.

[22] CHAUDHURI T., PHOK S., BHATTACHARYA R., *Thin Solid Films*, 515 (2007), 6971.

[23] VENKATESAN T., GREEN S.M., *TIP*, 2 (1996), 22.

[24] PENG R., XIA C., LIU X., PENG D., MENG G., *Solid State Ionics*, 152 – 153 (2002), 561.

[25] SHERRER P., *Göttinger Nachrichten Math. Phys.*, 2 (1918), 98.

[26] LALITHA S., SATHYAMOORTHY R., SENTHILARASU S., SUBBARAYAN A., NATARAJAN K., *Sol. Energ. Mat. Sol. C.*, 82 (2004), 187.

[27] PAL U., SAMANTHA D., GHORAI S., CHAUDHURI A.K., *J. Appl. Phys.*, 74 (1993), 6368.

[28] BHUIYAN M.R.A., ALAUDDIN M., AZAD A., HASAN S.M.F., *Indian J. Pure Ap. Phy.*, 49 (2011), 180.

[29] CHOUDHURY B., CHOUDHURY A., *Curr. Appl. Phys.*, 13 (2013), 217.

[30] RUIZ-TREJO E., *J. Phys. Chem. Solids*, 74 (2013), 605.

Received 2014-04-16
Accepted 2014-09-01